A New Technique for Magnetostatic Wave Delay Lines

MAKOTO TSUTSUMI, MEMBER IEEE, YOSHIHIKO MASAOKA, TAKASHI OHIRA, MEMBER, IEEE, AND NOBUAKI KUMAGAI, SENIOR MEMBER, IEEE

Abstract—A new technique for magnetostatic volume wave delay lines has been proposed where an inhomogeneous bias field is applied normal to the YIG slab surface and at transverse direction to the propagation of waves. Assuming an internal dc magnetic field in the raised cosine profile, theoretical time delay characteristics have been derived by a variational technique, and they have been confirmed with experiments by using a YIG slab oriented in a (110) plane. The large reductions on dispersion and loss have been highly significant.

I. Introduction

In recent years magnetostatic waves in a yttrium iron garnet (YIG) slab have found much interest for microwave device applications such as delay lines, filters, and resonators because of tunability and accessibility at surface of the YIG slab [1]. In general, the magnetostatic wave devices exhibit highly dispersive behavior and narrow bandwidth. The nondispersive magnetostatic volume and surface-wave delay lines composed of layered magnetic structures and a epitaxial YIG film have been investigated by several authors [2]–[4]. More recently, the authors have proposed a new technique to reduce the dispersive delay characteristic of the magnetostatic volume wave where an inhomogeneous bias field is applied normal to the YIG slab surface by using the artificially designed magnetic pole [5].

In this paper, the effects of an inhomogeneous bias field on the time delay characteristics of magnetostatic volume waves are studied theoretically by a variational technique, which are confirmed with experiments by using the YIG slab.

II. Theory

The analytical model is shown in Fig. 1. It consists of a lossless insulating YIG slab of thickness h lain in the x–y plane, sandwiched with perfect conductors. The bias field provided by a small rectangular electromagnet pole is applied inhomogeneously to the central portion of and normal to the YIG slab at transverse direction to the magnetostatic wave propagation (y direction).

First the dispersion relation of the magnetostatic waves is derived analytically assuming an internal dc magnetic field of the YIG slab in the step profile, i.e., an internal dc magnetic field strength is divided transversely into two regions, region I ($|x|>W/2$) and region II ($W/2>|x|$) as shown in Fig. 1(a). Secondly, the dispersion relation is estimated numerically by a variational technique where an internal dc magnetic field of the YIG slab in the raised cosine profile is assumed as shown in Fig. 1(b).

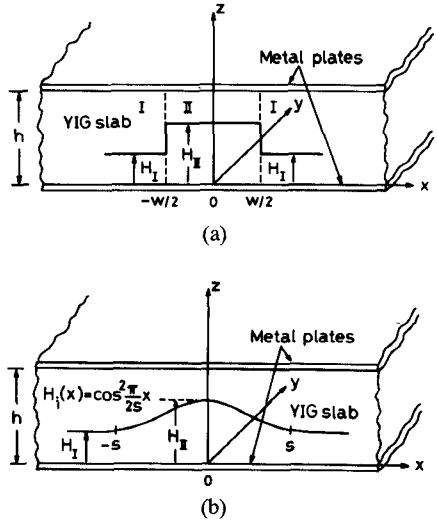

Fig. 1. Internal dc magnetic field model and coordinate system for analysis. (a) Step profile. (b) Raised cosine profile.

The relation between the magnetic flux and the RF magnetic field in the YIG medium can be expressed as [6]

$$\boldsymbol{B}=\mu_0\begin{pmatrix}\mu_{1j} & j\mu_{2j} & 0\\ -j\mu_{2j} & \mu_{1j} & 0\\ 0 & 0 & 1\end{pmatrix}\cdot\boldsymbol{H} \tag{1}$$

where the time dependence of fields is assumed to be $\exp(j\omega t)$, and

$$\mu_{1j}=\frac{(\gamma\mu_0)^2MH_j}{(\gamma\mu_0H_j)^2-\omega^2}+1$$

$$\mu_{2j}=\frac{\gamma\mu_0M\omega}{(\gamma\mu_0H_j)^2-\omega^2}. \tag{2}$$

In (2), the suffixes j, j=I and II, on the internal dc field H_j indicates the magnetic field strength in regions I and II, respectively, of Fig. 1(a). μ_0M is the saturation magnetization of YIG (1730 Oe), and $\gamma/2\pi$ is the gyromagnetic ratio (2.8 MHz/Oe).

Maxwell's equation under the quasistatic condition can

Manuscript July 23, 1980; revised December 1, 1980. This work was supported in part by the Research Fund of the Ministry of Education of Japan under Grant D-565118.

The authors are with the Department of Communication Engineering, Osaka University, Yamada Kami, Suita Osaka 564, Japan.

0018-9480/81/0600-0583$00.75 ©1981 IEEE

be expressed as

$$\nabla \times \boldsymbol{H} \simeq 0$$

and the RF magnetic field may be expressed in terms of scalar magnetic potential as

$$\boldsymbol{H} = -\nabla\phi. \tag{3}$$

By using (1)–(3) with Gauss' Law

$$\nabla \cdot \boldsymbol{B} = 0 \tag{4}$$

the magnetic potential is governed by the equation

$$\mu_{1J}\left(\frac{\partial^2\phi}{\partial x^2} + \frac{\partial^2\phi}{\partial y^2}\right) + \frac{\partial^2\phi}{\partial z^2} = 0. \tag{5}$$

Assuming that the magnetic potential ϕ_{I} in the region I decays exponentially in the x direction, and the magnetic potential ϕ_{II} in the region II varies sinusoidally across the high dc field region, the magnetic potentials in each region may be written as

$$\phi_{\mathrm{I}} = Ae^{+k_{\mathrm{I}}x}\cos\frac{n\pi}{h}ze^{\mp J\beta y} \qquad (x < -W/2) \tag{6a}$$

$$\phi_{\mathrm{II}} = \left(C\cos k_{\mathrm{II}}x + D\sin k_{\mathrm{II}}x\right)\cos\frac{n\pi}{h}ze^{\mp J\beta y} \qquad (-W/2 < x < W/2) \tag{6b}$$

and

$$\phi_{\mathrm{I}} = Be^{-k_{\mathrm{I}}x}\cos\frac{n\pi}{h}ze^{\mp J\beta y} \qquad (x > W/2) \tag{6c}$$

where β and n are the propagation constant and the magnetostatic wave resonance number in the z direction, respectively. Transverse propagation constants k_{I} and k_{II} are obtained from (5) as

$$k_{\mathrm{I}} = \sqrt{\frac{1}{\mu_{1\mathrm{I}}}\left(\frac{n\pi}{n}\right)^2 + \beta^2}$$

$$k_{\mathrm{II}} = \sqrt{\frac{1}{-\mu_{1\mathrm{II}}}\left(\frac{n\pi}{h}\right)^2 - \beta^2}. \tag{6d}$$

Equation (6) is satisfied with the boundary conditions of metal plates in the z direction.

The boundary conditions in the transverse direction are

$$\phi_{\mathrm{I}} = \phi_{\mathrm{II}} \qquad (x = \pm W/2) \tag{7}$$

for continuity of the tangential component of the RF magnetic field, and

$$B_{x\mathrm{I}} = B_{x\mathrm{II}} \qquad (x = \pm W/2) \tag{8}$$

for continuity of the normal component of the magnetic flux density. Substituting (6) into the boundary conditions (7) and (8) and eliminating the constants A, B, C, and D in (6), we obtain the dispersion relation for the magnetostatic volume wave mode (SVS mode)

$$\tan k_{\mathrm{II}}W = \frac{2\mu_{1\mathrm{II}}\mu_{1\mathrm{III}}k_{\mathrm{I}}k_{\mathrm{II}}}{(\mu_{2\mathrm{I}} - \mu_{2\mathrm{II}})^2\beta^2 - \mu_{1\mathrm{II}}^2k_{\mathrm{I}}^2 + \mu_{1\mathrm{III}}^2k_{\mathrm{II}}^2}. \tag{9a}$$

If k_{II} in (6b) has the imaginary value, we could obtain the dispersion relation of the magnetostatic surface wave mode (SSS mode) from (9a)

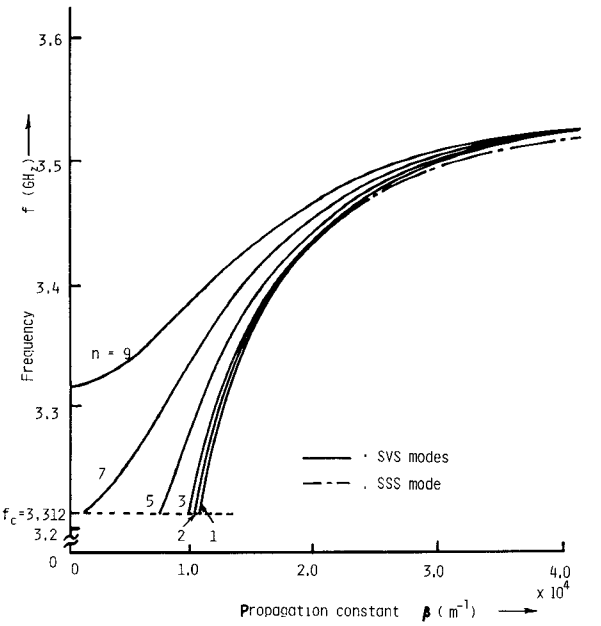

Fig. 2. Dispersion diagrams of magnetostatic volume and surface wave modes as a function of the transverse resonant number.

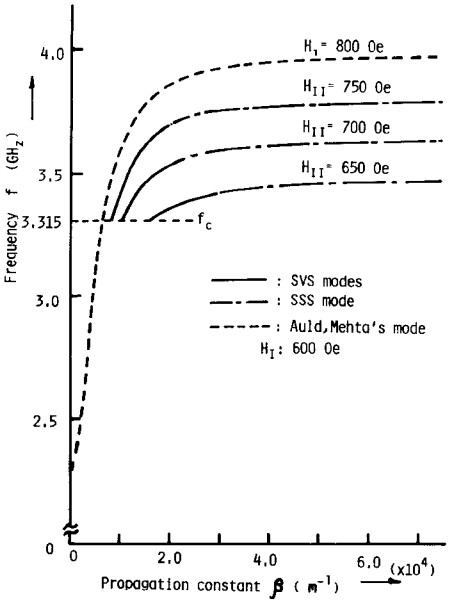

Fig. 3. Dispersion diagrams for different values of an internal dc magnetic field in the step profile.

$$\tanh k'_{\mathrm{II}}W = \frac{2\mu_{1\mathrm{II}}\mu_{1\mathrm{III}}k_{\mathrm{I}}k'_{\mathrm{II}}}{(\mu_{2\mathrm{I}} - \mu_{2\mathrm{II}})^2\beta^2 - \mu_{1\mathrm{II}}^2k_{\mathrm{I}}^2 - \mu_{1\mathrm{III}}^2k'^2_{\mathrm{II}}} \tag{9b}$$

where $k'_{\mathrm{II}} = -jk_{\mathrm{II}}$.

The dispersion relations of (9) can be estimated numerically. The typical dispersion diagrams of SVS and SSS modes are shown in Figs. 2 and 3 where a slab thickness of 0.5 mm, an internal magnetic field in the region I of 600 Oe and the width of region II of 2 mm are assumed. The dispersion diagram of Fig. 2 is shown as a function of the resonance number n where H_{II} is assumed to be 700 Oe. With reference to Fig. 2, it should be noted that the dispersion curve of the SVS mode with solid lines connects smoothly the curve of the SSS mode with the chain line at

high frequencies. The dispersion diagram of Fig. 3 is shown as a function of an internal dc magnetic field in the step profile where H_I of 600 Oe and the fundamental resonance mode $n=1$ are assumed. As seen in the figure the broken line represents the dispersion diagram of the magnetostatic volume mode in the YIG slab with metal boundaries discussed by Auld and Mehta [7] where an internal magnetic field is assumed to be uniform. It is shown that the slope $\partial f/\partial\beta$ of dispersion curves of Fig. 3 decreases with decreasing the magnetic field strength H_{II}. Thus the reduction of the dispersive group delay characteristics of the magnetostatic waves may be achieved by choosing a moderate strength of the bias field in the region II.

An internal dc magnetic field in the step profile is not realistic form. It is natural to assume an internal field in the raised cosine profile. With the help of a variational technique, which is one of a well-known approximation technique, the dispersion characteristics of this case are estimated numerically where magnetostatic wave fields in the case of an internal dc field in the step profile are chosen as a trial field.

Assuming that the magnetic potential and magnetic flux in (3) and (4) vary as $\exp(-j\beta y)$, they satisfy the equation

$$\nabla_t\cdot\hat{\boldsymbol{B}}(x,z)-j\beta\hat{\boldsymbol{B}}(x,z)\cdot\boldsymbol{i}_y=0 \tag{10}$$

$$\hat{\boldsymbol{H}}=-\nabla_t\hat{\phi}(x,z)+j\beta\hat{\phi}(x,z)\cdot\boldsymbol{i}_y \tag{11}$$

where ∇_t is the two-dimensional operator, $\hat{\phi}$ and $\hat{\boldsymbol{B}}$ are a function of the transverse direction for the wave propagation, and $\boldsymbol{i}_y$ is the unit vector for the propagation direction.

We take the scalar product of $\hat{\phi}$ with (10) and $\boldsymbol{B}^*$ with (11) where the asterisk denotes the complex conjugate of fields. Taking the sum of above two equations and integrating the result over the cross section of the magnetostatic wave guide shown in Fig. 1(b), we get

$$\beta=\frac{\int_{-\infty}^{+\infty}\int_0^h\left[\hat{\mu}^*(x)\cdot\hat{\boldsymbol{H}}^*\cdot\hat{\boldsymbol{H}}+\hat{\mu}^*(x)\cdot\hat{\boldsymbol{H}}^*\cdot\left(\nabla_t\hat{\phi}\right)+\hat{\mu}(x)\cdot\hat{\boldsymbol{H}}\cdot\left(\nabla_t\hat{\phi}^*\right)\right]dz\,dx}{j\int_{-\infty}^{+\infty}\int_0^h\boldsymbol{i}_y\cdot\left[\hat{\phi}\hat{\mu}^*\cdot\hat{\boldsymbol{H}}^*-\hat{\phi}^*\hat{\mu}(x)\cdot\hat{\boldsymbol{H}}\right]dz\,dx} \tag{12}$$

where $\boldsymbol{B}\cdot\boldsymbol{n}=0$ is considered since the normal component of the magnetic flux must vanish at the metal boundaries of the magnetostatic wave guide. Equation (12) is the variational formula for the propagation constant of the magnetostatic wave. A stationary character of the formula can be easily proved by putting the first variation of trial fields $\delta\boldsymbol{H}$ and $\delta\phi$ (see Appendix). In Equation (12), the magnetic suceptibility $\mu(x)$ is a function of an internal dc magnetic field $H_i(x)$ in the transverse direction. We assume the dc magnetic field distribution in the form of

$$H_i(x)=(H_{II}-H_I)\cos^2\frac{\pi}{2s}x+H_I \tag{13}$$

where H_{II} is the maximum value of the dc field in the raised cosine profile. The parameter s expresses the extent of the raised cosine profile shown in Fig. 1(b). The parameter s can be determined numerically by choosing that the integration of (13) with respect to x

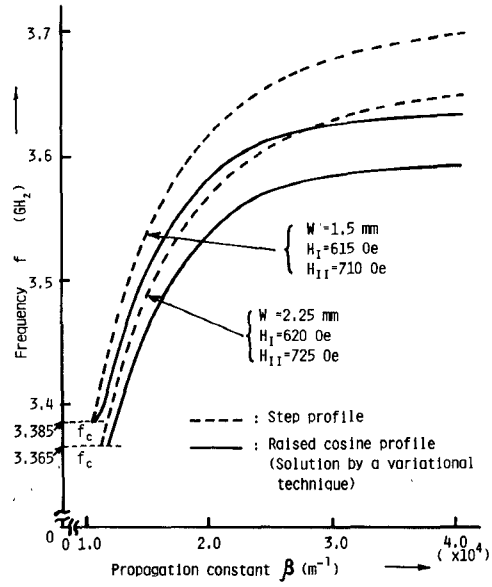

Fig. 4. Dispersion diagrams for different values of an internal dc magnetic field in the raised cosine profile.

$$\int_{-s}^{s}(H_{II}-H_I)\cos^2\frac{\pi}{2s}x\,dx=\Delta s_1$$

is equal to the integration of the dc field in the step profile

$$W(H_{II}-H_I)=\Delta s_1.$$

Substituting the (1), (2) with (13) and the trial fields of SVS mode of (6) into (12), the variational formula is calculated numerically. Typical dispersion diagram is shown in Fig. 4. To demonstrate clearly the effect on the dc magnetic field in the raised cosine profile the dispersion curves for dc field in the step profile (solution of (9a)) are also depicted with dotted lines in Fig. 4 where n is assumed to be unity and other numerical values are written in the figure. With comparison between those curves, the propagation characteristics in the raised cosine profile become more dispersive than that of the dc field in the step profile. The dispersion curves of Fig. 4 are provided to assess the experimental results which will be discussed in the next section.

III. Experiments

The YIG slab used for the experiment is a polished single crystal ($0.56\times0.45\times0.056$ in·cm) oriented in the (110) plane. The slab is sandwiched by copper plates. The pole of the electromagnet of the delay line is artificially designed in order to magnetize inhomogeneously the central portion of the YIG slab [5]. A small iron round or rectangular pole piece is attached to the main pole of the electromagnet and it is separated with about 1.5-mm air gap from the YIG. Two different round pole pieces of diameter 1.2

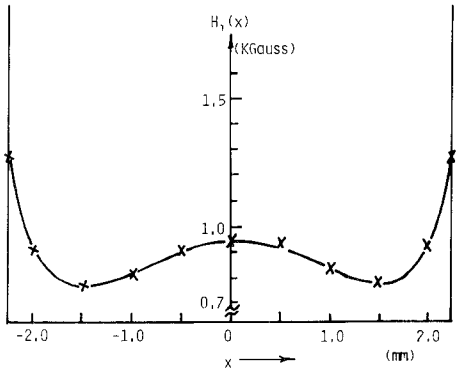

Fig. 5. Internal dc magnetic field profile in a perpendicularly magnetized YIG slab by the sharpened electromagnet pole.

and 3.3 mm, and three different rectangular pole pieces having cross section of 4.3×2.0, 0.3×4.75, and 0.25×4.75 mm^2 are tested. The dc field distributions formed by these sharpened poles in the air-gap region were measured by Hall-effect magnetometer where they showed the raised cosine profile [5].

The magnetic field strength within YIG slab may be different from that of air region due to the demagnetizing effect. The perpendicular demagnetizing factor for a rectangular geometry of sample biased normal to the broad surface is given by [8]

$$N_{zz}=\frac{1}{4\pi}\{\cot^{-1}f(x,y,z)+\cot^{-1}f(x,y,-z)+\cot^{-1}f(x,-y,z)+\cot^{-1}f(x,-y,-z)+\cot^{-1}(-x,y,z)+\cot^{-1}f(-x,y,-z)+\cot^{-1}f(-x,-y,z)+\cot^{-1}f(-x,-y,-z)\} \quad (14)$$

where

$$f(x,y,z)=\frac{\{(x-a)^2+(y-b)^2+(z-c)^2\}^{1/2}(c-z)}{(x-a)(y-b)}$$

and a, b, and c are dimensions of sample. The relation between the applied field $H_0(x)$ and the internal field $H_i(x)$ is given by

$$H_i(x)=H_0(x)-4\pi MN_{zz}. \quad (15)$$

An internal dc magnetic field profile as a function of the transverse direction x, calculated from (15), is shown in Fig. 5 where the measured value of the dc field by a Hall-effect magnetometer is used as $H_0(x)$ [5], a, b, and c are 0.45, 0.56, and 0.056 in·cm, respectively. If the contribution to the magnetostatic wave for slab edges is neglected because of the cut off character of wave at high dc field, we could expect that an internal dc field formed by the sharpened pole shows the raised cosine profile, even if the demagnetizing effect exists. As seen from the figure the difference between the maximum and minimum values of an internal dc field in the raised cosine profile is evaluated to be about 200 Oe.

Experiments for group delay are carried out by using a microwave signal of about 3.5 GHz modulated by the p-i-n diode of 0.1-μs pulsewidth [5]. The measured time delay characteristics as a function of frequency are shown in Fig. 6 where Fig. 6(a) and (b) correspond to the experimental results for the round and rectangular magnetic poles, respectively. In those experiments, the maximum value of the bias field in the raised cosine profile $H_{0\max}$ is adjusted so as to obtain a time delay of 0.1 μs at 3.4 GHz. The theoretical results are also depicted in Fig. 6 with solid lines in which the numerical values used for the calculation are shown in the figure. Theoretical curves in Fig. 6(a) are estimated numerically from the gradient of the dispersion curves of Fig. 4, which are calculated by a variational technique. It should be noted in Fig. 6 that the experimental results agree reasonably well with the theoretical predictions and that the theoretical form of an internal dc field ($H_{II}-H_I \simeq 100$ Oe and $s \simeq 3$ mm) approaches the internal dc field profile shown in Fig. 5. Also the experimental and theoretical results of the time delay for the flat pole piece (homogeneous bias field) are plotted in Fig. 6(a). For the flat pole the time delay more than 0.25 μs could not be detected because of highly dispersive behavior, but the theoretical curve with the dotted line, calculated from Auld and

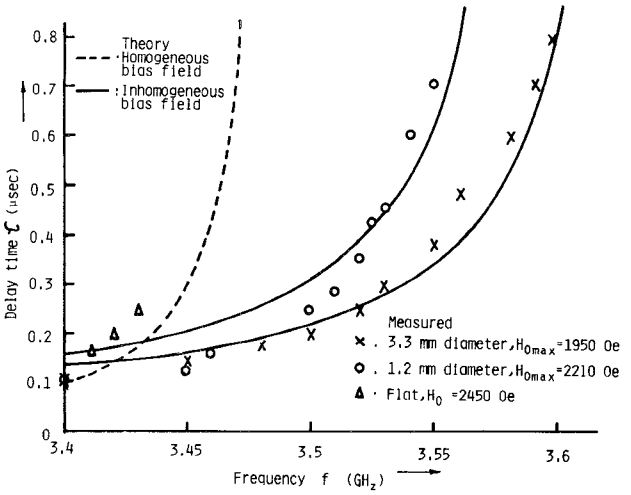

(a)

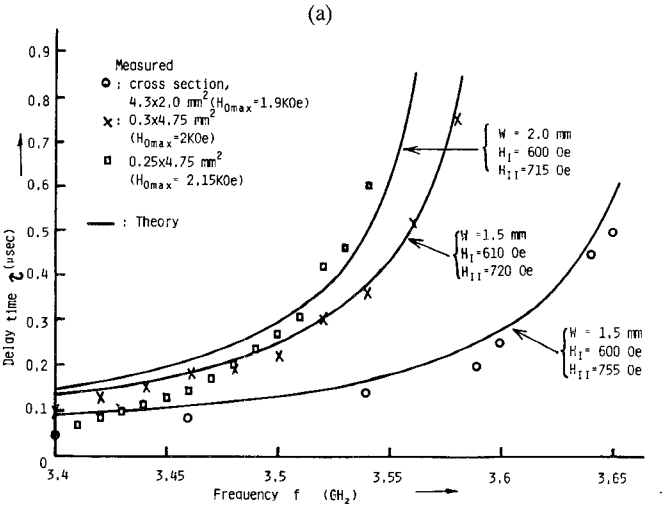

(b)

Fig. 6. Measured and calculated group delay characteristics as a function of frequency. (a) Round pole piece. (b) Rectangular pole piece.

Mehta's dispersion relation [7], coincides with the experimental result. It is interesting to note that the frequency bandwidth of the time delay is several times wider than that of the flat pole. Comparatively, a more broad-band characteristic of the group delay may be achieved by providing carefully designed sharpened magnetic pole.

Throughout the experiments we have examined the possibility of the excitation of the SSS mode or higher modes of the SVS mode, but those modes could not be found experimentally in our antenna configuration [5].

The propagation loss as a function of the time delay is also examined experimentally. The average value of the propagation loss in the case of an inhomogeneous bias field is found to be about 30 dB/μs which is several tens of decibels lower than that of the homogeneous bias field case [5]. When the sample is magnetized by the sharpened pole, the magnetostatic potential distributes sinusoidally in the high dc field region and exponentially in the low dc field of side regions as mentioned in (6). The magnetostatic wave energy will be guided along the high dc field region. As a consequence, the scattering of the SVS mode beam at the corners and edges of the YIG slab will be largely prevented. Thus the large reduction on loss becomes significant. This is along with the same principle of the high-Q YIG resonator using nonuniformly magnetized YIG slab, which has been investigated by Zeskind and Morgenthaler [9], [10].

IV. Conclusion

A new technique for magnetostatic volume wave delay lines, in which an inhomogeneous bias field is applied normal to the surface of the YIG slab, has been proposed, and investigated both theoretically and experimentally. Under the magnetostatic approximation of the Maxwell's equations, the variational formula of the propagation constant of the magnetostatic waves has been derived. The formula is estimated numerically assuming that an internal dc magnetic field in the YIG slab distributes in the raised cosine profile and that the field solutions in the dc magnetic field in the step profile are chosen as a trial field. The reduction of dispersive characteristics of the time delay has been shown in several dispersion diagrams as a function of an internal magnetic field profile.

The experiments on the time delay of the magnetostatic volume wave (SVS mode) have been carried out by using a polished single crystal of YIG slab oriented (110) plane where the central portion of the slab is magnetized inhomogeneously by the sharpened magnetic pole. The frequency bandwidth of the time delay is found to be about three times wider than that of the flat pole where it has been good agreement with theory. The propagation loss, as opposed to homogeneous bias fields, has been significantly reduced.

If we apply this technique to an expitaxial grown YIG film. One would suspect that fairy low dispersion of the time delay might be possible.

Appendix

We set

$$\beta=\beta_0+\delta\beta \qquad \boldsymbol{H}=\boldsymbol{H}_0+\delta\boldsymbol{H} \qquad \phi=\phi_0+\delta\phi \quad \text{(A-1)}$$

where $\delta\beta$, $\delta\boldsymbol{H}$, and $\delta\phi$ are the first variation of β_0, $\boldsymbol{H}_0$, and ϕ_0, respectively. Substituting (A-1) into (12), we obtain

$$j\delta\beta\int_s(\phi_0\boldsymbol{B}_0^*-\phi_0^*\boldsymbol{B}_0)\,ds=S_1+S_2+S_3+S_4 \quad \text{(A-2)}$$

where

$$S_1=\int_s\hat{\mu}\cdot\delta\boldsymbol{H}\cdot(\boldsymbol{H}_0^*+\nabla_t\phi_0^*+j\beta\phi_0^*\cdot\boldsymbol{i}_y)\,ds$$

$$S_2=\int_s\hat{\mu}^*\cdot\delta\boldsymbol{H}^*\cdot(\boldsymbol{H}_0+\nabla_t\phi_0-j\beta\phi_0\cdot\boldsymbol{i}_y)\,ds$$

$$S_3=\int_s-\delta\phi(\nabla_t\cdot\boldsymbol{B}_0^*+j\beta\boldsymbol{i}_y\cdot\boldsymbol{B}_0^*)\,ds+\int_c\delta\phi\boldsymbol{B}^*\cdot\boldsymbol{n}\,dl$$

$$S_4=\int_s-\delta\phi^*(\nabla_t\boldsymbol{B}_0-j\beta\boldsymbol{i}_y\cdot\boldsymbol{B}_0)\,ds+\int_c\delta\phi^*\boldsymbol{B}\cdot\boldsymbol{n}\,dl.$$

S_1, S_2, S_3, and S_4 in (A-2) will vanish with the help of (10) and (11), together with the boundary condition of $\boldsymbol{B}\cdot\boldsymbol{n}=0$. Consequently, the right-hand side of (A2) vanishes. This leads a stationary character of the propagation constant, i.e., $\delta\beta=0$.

Acknowledgment

The authors wish to thank Prof. F. R. Morgenthaler for stimulating discussions of the research on magnetostatic modes bound by dc-field gradients carried out at Massachusetts Institute of Technology during his recent visit to Osaka University.

References

[1] J. D. Adam and J. H. Collins, "Microwave magnetostatic delay devices based on expitaxial yttrium iron garnet," *Proc. IEEE*, vol. 64, pp. 794–800, May 1976.

[2] N. S. Chang and Y. Matsuo, "Numerical analysis of MSSW delay line using layered magnetic thin slabs," *Proc. IEEE*, vol. 66, pp. 1577–1578, Nov. 1978.

[3] N. D. J. Miller, "Nondispersive magnetostatic volume wave delay line," *Electron. Lett.*, vol. 12, pp. 466–467, Sept. 1976.

[4] M. R. Daniel, J. D. Adam, and T. W. O'Keeffe, "Linearly dispersive magnetostatic delay line at X band," *IEEE Trans. Magn.*, vol. MAG-15, pp. 1735–1737, Nov. 1979.

[5] M. Tsutsumi, Y. Masaoka, T. Ohira, and N. Kumagai, "The effect on an inhomogeneous bias field on the delay characteristics of magnetostatic forward volume waves," *Appl. Phys. Lett.*, vol. 35, pp. 204–206, July 1979.

[6] R. W. Damon and J. R. Eshbach, "Magnetostatic modes of a ferromagnet slab," *J. Phys. Chem. Solids*, vol. 19, pp. 308–320, 1961.

[7] B. A. Auld and K. B. Mehta, "Magnetostatic waves in a transversely magnetized rectangular rod," *J. Appl. Phys.*, vol. 38, pp. 4081–4083, 1967.

[8] R. I. Joseph and E. Schlomann, "Demagnetizing field in nonellipsoidal bodies," *J. Appl. Phys.*, vol. 36, pp. 1579–1593, May 1965.

[9] D. A. Zeskind and F. R. Morgenthaler, "Localized high Q ferromagnetic resonance in nonuniform magnetic fields," *IEEE Trans. Magn.*, vol. MAG-13, pp. 1249–1251, Sept. 1977.

[10] F. R. Morgenthaler, "Novel devices based upon field gradient control of magnetostatic modes and waves," presented at the 3rd Int. Conf. Ferrites, Kyoto Japan, Sept. 29–Oct. 2, 1980.